On the theory of the steady perturbations in the troposphere

By JOSEF EGGER, *Institut für Theoretische Meteorologie der Universität München, München, FRG*

(Manuscript received November 10, 1975)

ABSTRACT

The linear steady-state response of a hemispheric two-level primitive equation model to forcing by heat sources and by topography is studied. Realistic forcing is considered for January where the zonal variation of the release of latent heat and of the sensible heating dominates the radiational heating. The response to each of these heat sources is discussed and an attempt is made to understand the computed patterns by aid of a simple quasigeostrophic theory. The combined topographical and thermal forcing induces standing waves which verify favourably against observations. At 400 mb, the ridge on the windward side of the Himalayas and the trough over north-eastern Asia appear to be induced by the orography whereas the heat sources play an almost dominant role over North America and determine the position of the ridge over the Atlantic. At 800 mb, the linear model fails to simulate the Aleutean low but is rather satisfactory elsewhere. The northward transport of heat and momentum by the standing waves is discussed.

1. Introduction

In a previous paper by the writer (1976), hereafter referred to as I, the linear steady response of a hemispheric primitive equation model to forcing by topography has been presented. The main purpose of the present paper is to give the results obtained by including heating functions.

The heat sources in the model have been incorporated by use of the observed time-averaged fluxes of sensible heat and long-wave radiation at the boundaries of the atmosphere and of the observed patterns of the release of latent heat. This approach allows us to compute separately the influence of the various forcing terms on the standing planetary waves. We shall restrict our analysis to the case of January mean conditions.

As in I, an attempt will be made to qualitatively understand the gross features of the computed response by use of a simple quasigeostrophic theory.

2. The model

The formulation of the basic equations of our two-level model is given in I. Fig. 1 shows the layering and the grid points of the model. The equations of horizontal motion, the thermodynamic energy equation, the continuity equation, all written for 400 mb and 800 mb, and the tendency equation of the height of the 1 000 mb surface constitute the set of equations of the model. The equations are expressed in a steady-state linearized form where the prescribed basic state is assumed independent of longitude and time. All perturbation quantities are expanded in longitudinal Fourier series up to and including wavenumber eight. The expansion coefficients are the variables of the model. We expand the horizontal wind and the temperature perturbation at 400 mb and at 800 mb, the ω-perturbation at 600 mb and 1 000 mb and the perturbation of the 1 000-mb height. The model includes surface friction and the vertical transfer of momentum due to the vertical shear of the horizontal wind. The orography is incorporated via the conventional formulation, i.e. we have a forced vertical motion at the 1 000 mb surface. The various sources of heating are prescribed according to observations.

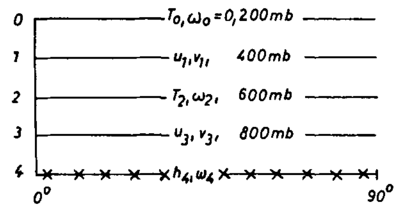

Fig. 1. Schematic representation of the structure of the primitive equation model. The grid points of the model are marked by crosses.

3. Response to forcing in a quasigeostrophic two-layer model

In I, the writer made an attempt to explain the response of the primitive equation-model to forcing by topography by use of a conventional quasigeostrophic two-level model with β-plane approximation. It turned out that several features of the computed results could be understood at least qualitatively by aid of this simple model. Here, we shall try to expand this analysis to the forcing by heat sources and orography.

In the quasigeostrophic theory, the basic equations of the primitive equation model are replaced by the linearized steady-state vorticity equation at 400 mb (subscript 1) and at 800 mb (subscript 3) on the β-plane and by the thermodynamic energy equation at 600 mb (subscript 2). They are written

$$\bar{u}_1 \frac{\partial}{\partial x} \nabla^2 \phi_1 + \beta \frac{\partial \phi_1}{\partial x} = f_0^2 \frac{\omega_2}{Dp} \tag{1}$$

$$\tfrac{1}{2}(\bar{u}_1 + \bar{u}_3) \frac{\partial}{\partial x} (\phi_3 - \phi_1) + \tfrac{1}{2} \frac{\partial}{\partial x} (\phi_1 + \phi_3)(\bar{u}_1 - \bar{u}_3) + \omega_2 \sigma Dp = -QDp \tag{2}$$

$$\bar{u}_3 \frac{\partial}{\partial x} \nabla^2 \phi_3 + \beta \frac{\partial \phi_3}{\partial x} = f_0^2(\omega_4 - \omega_2)/Dp \tag{3}$$

where the notation is conventional. σ is the static stability, $Dp = 400$ mb. Here, the zonal wind velocity $\bar{u}$ of the basic flow does not depend on the latitude. Q represents the heating. To simplify the discussion, we have excluded all friction terms. The vertical motion at 1 000 mb (subscript 4) is given by

$$\omega_4 = -g \bar{\varrho}_4 \bar{u}_4 \frac{\partial}{\partial x} H \tag{4}$$

where H is the topographic profile.

Expanding the variables and the forcing terms in double Fourier series, e.g.

$$\phi_1 = \mathrm{Re} \left\{ \sum_{m,n} \phi_{1mn} \exp\left(2\pi i(mx/L_x + ny/L_y)\right) \right\} \tag{5}$$

where L_x, L_y are the largest wave-lengths in x and y we obtain the solution

$$\phi_{1mn} = (\bar{u}_1 \alpha_c M_{mn} - i(\bar{u}_3 \alpha - \beta)\hat{Q}_{mn})/D \tag{6}$$

$$\phi_{3mn} = ((\bar{u}_1 \alpha + \bar{u}_3 \alpha_c - \beta) M_{mn} - i(\beta - \bar{u}_1 \alpha)\hat{Q}_{mn})/D \tag{7}$$

where

$$\hat{Q}_{mn} = \alpha_c Dp L_x Q_{mn}/2\pi$$

$$\alpha = 4\pi^2(m^2/L_x^2 + n^2/L_y^2)$$

$$\alpha_c = f_0^2/(\sigma Dp^2)$$

$$M_{mn} = \bar{u}_4 \bar{\varrho}_4 g f_0^2 H_{mn}/Dp$$

$$D = \bar{u}_1 \bar{u}_3 \alpha^2 + ((\bar{u}_1^2 + \bar{u}_3^2)\alpha_c - \beta(\bar{u}_1 + \bar{u}_3))\alpha + \beta(\beta - (\bar{u}_1 + \bar{u}_3)\alpha_c) \tag{8}$$

The first terms on the right hand sides represent the response to topographic forcing which has been discussed in I. Here, we shall turn to the second terms which give the perturbations excited by the heat sources. Obviously, the perturbation geopotential is out of phase by $\pm\pi/2$ with the heat source. In most cases, we have to expect a node between 400 mb and 800 mb, i.e. ϕ_{1mn} and ϕ_{3mn} have different signs. The only exceptions are for $\beta/\bar{u}_1 > \alpha > \beta/\bar{u}_3$ and $\beta/\bar{u}_3 > \alpha > \beta/\bar{u}_1$. This is in agreement with the computations of Saltzman (1965) who found a node at about 700–500 mb in most of his solutions.

It is more difficult to assess the signs of ϕ_{1mn}, ϕ_{3mn} since we have to know the sign of D. This problem has been discussed in I. Here, we shall concentrate on the January flow in middle latitudes and use the results obtained in I. Most of the topographical forcing as well as most of the zonal variation of the heating functions occur at wave number two. The meridional wavelength of the forcing functions can be assumed 90°. It has been shown that $D < 0$ under these conditions (so-called ultralong waves; see Table 2 of I). Furthermore, we have $\beta/\bar{u}_1 > \alpha$, $\beta/\bar{u}_3 > \alpha$ at middle latitudes. Hence, we have to expect a trough downstream of the heating sources at 800 mb and a ridge at 400 mb. The displacement should amount to about one

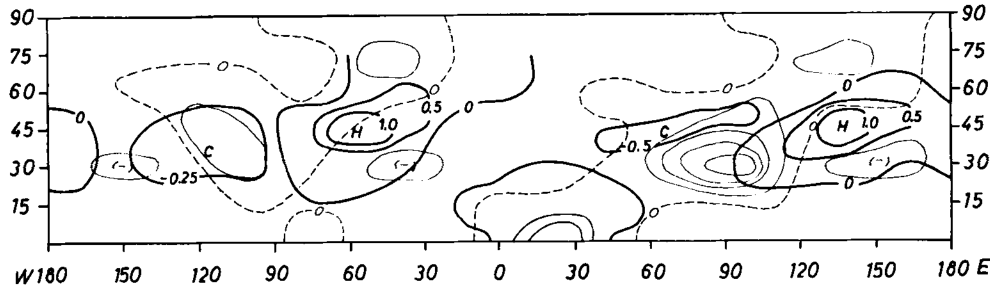

Fig. 2. Heating of the lower layer (1 000–600 mb) of the primitive equation model due to the flux of sensible heat at the earth's surface for January (K day^{-1}). The thin lines represent the orography with isolines every 500 m and the 0 m contour dashed.

quarter of the wavelenght. However, we have $\beta/\bar{u}_1 < \alpha$ for $m \gtrsim 3$. Therefore, the response in the lower layer will show a ridge downstream for $m \gtrsim 3$ or for smaller meridional wavelengths.

It is known from observations that the transports by the standing planetary waves play a significant role in the heat and momentum budget of the general circulation of the atmosphere. Let us look at the zonally averaged transport of sensible heat at 600 mb in the quasi-geostrophic model. By (6), (7) we have

$$v_2 = \sum_m \frac{i\pi m}{L_x f_0 D} ((\bar{u}_1 + \bar{u}_3)\alpha_c + \bar{u}_1 \alpha - \beta) M_m - i\hat{Q}_m(\bar{u}_3 - \bar{u}_1)\alpha) e^{2\pi i m x/L_x} \tag{9}$$

The hydrostatic relation yields

$$T_2 = 3(\phi_1 - \phi_3)/(2R) \tag{10}$$

Hence,

$$T_2 = \sum_m \frac{3}{2RD} [(\bar{u}_1(\alpha_c - \alpha) - \bar{u}_3 \alpha_c + \beta) M_m - i\hat{Q}_m((\bar{u}_1 - \bar{u}_3)\alpha - 2\beta)] e^{2\pi i m x/L_x} \tag{11}$$

where the factor $e^{2\pi i n y/L_y}$ has been omitted in (9) and (11) since the computation of the northward transport of sensible heat does not involve derivatives in y. After simple algebraic manipulations, the zonally averaged transport of sensible heat is found to be

$$\frac{1}{L_x}\int_0^{L_x} (vT)_2\, dx = -\sum_m \frac{3\pi m}{2Rf_0 L_x D}[M_m Q_m^* + Q_m M_m^*], \tag{12}$$

where the star denotes the complex conjugate.

This is a result of remarkable simplicity. Standing waves which are excited in frictionless flow by orography or heating alone do not transport sensible heat. Both forcing functions must be combined. There are no transports of heat when the orography and the heating are out of phase by $\pm\pi/2$ and we have to expect maximum transport when both are in phase or out of phase by π. The direction of the transports is dictated by the relative position of the topography and the heat sources and by the sign of D. If applicable to the general circulation (12) would greatly increase our understanding of the observed transports by standing waves in the atmosphere. However, the incorporation of the surface friction influences strongly the position of the forced waves and, therefore, the transport properties. It has been shown in I, that the standing waves shifted towards the east by about 50–90° longitude when surface friction was included. One can try to include the surface friction into the quasigeostrophic theory. It can be shown, then, that the standing waves which are induced by heating can transport heat by themselves once surface friction is taken into account. The resulting formulae for the composite transport are rather complicated and are not presented here. (12) predicts southward transport of sensible heat at wave-number two in the middle latitudes when observed values of Q_2 and M_2 are inserted whereas the linear model gives southwards transport north of 45° N and northward transport south of 45° N (see Fig. 13).

4. Results

In the sequel, we shall present the response of the two-level model to prescribed heat sources

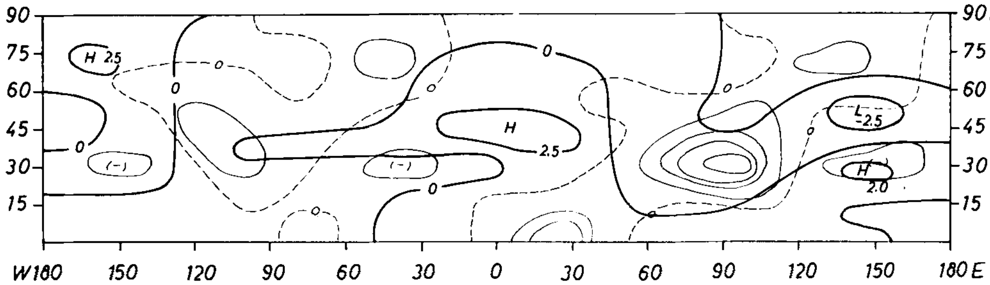

Fig. 3. Perturbation of the 400 mb height (dm) by sensible heat forcing for January.

and topography for January conditions. The January basic state has been taken from Oort & Rasmusson (1971) and is identical to that used in I. If not stated otherwise, surface friction, the vertical shear stress and the mean meridional motion of January have been included in the computations.

The following heat sources have been incorporated:

(i) Heating due to the flux of sensible heat at the earth's surface. The January fluxes have been taken from Gates (1972) after Budyko (1963).

(ii) Heating due to the release of latent heat. The data have been taken from the precipitation charts for December–February as given by Gates (1972) after Möller (1951).

(iii) Heating due to long-wave radiation. The fluxes of long-wave radiation at the lower boundary of the atmosphere have been taken from Gates (1972) and the outgoing long-wave radiation emitted to space from Raschke et al. (1973). The data of Raschke et al. cover the period January 21 to February 3, 1970.

(a) Response to the heating by the flux of sensible heat at the earth's surface

Fig. 2 shows the deviation of the heating from the zonal average in the lower layer of the model due to the flux of sensible heat from the earth's surface. The variations in the heating are primarily due to the ocean currents. Major heat sources are found off the east coast of North America and Asia. The continents act as sinks in January. It has been assumed that the sensible heat flux is absorbed by the lower layer only (see also, Newell et al., 1969, Fig. 7).

Fig. 3 shows the perturbation of the height of the 400 mb-surface as enforced by this heating distribution in the model. Wavenumbers 1–2 dominate the response. There is an area of high pressure over the eastern Atlantic and Europe downstream of the Gulf Stream heating. Low pressure is found beneath at 800 mb but somewhat displaced towards the north-east (Fig. 4). This is in agreement with the quasigeostrophic theory which predicts high pressure downstream of the heat source at the upper level for ultra-long waves. However, it has been shown in I,

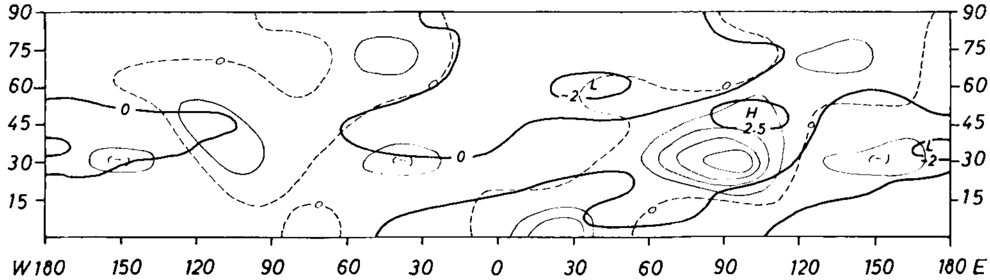

Fig. 4. Perturbation of the 800 mb height (dm) by sensible heat forcing for January.

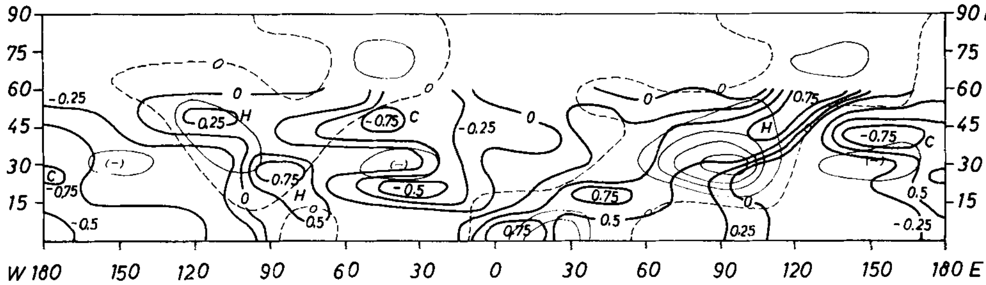

Fig. 5. Heating of the troposphere (1 000–200 mb) due to the fluxes of longwave radiation at the boundaries of the atmosphere for January (K day^{-1}).

that the incorporation of friction may cause an eastward shift of the standing waves by almost half a wavelength at wavenumber two. Indeed, a further experiment without friction predicted a low with its center at 10° W, 40° N at 400 mb at wavenumber two but a high farther north. Hence, the response is too complicated to be guessed from (6), (7). Further experiments with simply distributed heat sources revealed that the response at midlatitudes is in fair agreement with the quasigeostrophic theory outlined above. However, the heating pattern of Fig. 2 involves so many meridional wavenumbers that a verification of the quasigeostrophic theory could be achieved at best by a superposition of many Fourier modes. This has not been attempted. Over the Pacific, we observe a long band of low pressure downstream of the warming at 800 mb, but the corresponding ridge at 400 mb is extremely weak. A closer analysis reveals that a ridge is induced at 400 mb downstream of the Pacific warming at wavenumber two which is, however, almost completly owerpowered in Fig. 3 by the reverse response at wavenumber one. The transports of sensible heat and westerly momentum by the waves shown in Figs. 3, 4 are rather weak.

(*b*) *Response to the release of latent heat*

The heating pattern created by the release of latent heat is similar to that due to the flux of late sensible heat from the earth's surface. Two experiments have been made. In the first experiment, it has been assumed that all the latent heat is released in the lower layer of the model. In the second one, the heating in the lower layer is given by $Q(1-\cos^4 \varphi)$ and by $Q \cos^4 \varphi$ in the upper layer where φ is the latitude and Q the observed heating. The latter experiment has been carried out in order to approximate the observed variation of the height of maximum heat release with latitude (see Fig. 7 of Newell et al., 1969). Except minor details, the result was the same in both experiments and the more realistic formulation has been used in all following experiments.

At 400 mb, the response is somewhat stronger than in the sensible heating experiment. In particular, there is now a strong ridge (5 gpdm) over Alaska where only a small area of high pressure could be seen in Fig. 3 and the low pressure system over eastern Canada is connected with that over the northern Pacific. The pattern over the Atlantic is much the same as in Fig. 3. At 800 mb, the response pattern is also very similar to that shown in Fig. 4 but has double the amplitude. Again, the transports are almost vanishing.

We can state that the flux of sensible heat and the release of latent heat tend to create the same type of response in January. The latter, however, has a stronger amplitude.

(*c*) *Response to longwave radiation*

Fig. 5 shows the zonal variation of the heating of an atmospheric column due to longwave radiation as compiled from the charts of Gates (1972) and Raschke et al. (1973). In general, we have relative heating over the cold continents and relative heat losses over the oceans. Hence, the longwave heating pattern is fairly opposite to that due to the flux of sensible heat and the release of latent heat. Of course, it is the same with the response of the model (Fig. 6), where the same amount of longwave heating has been allotted to each of the two layers of the model.

We have low pressure over the Atlantic at 400 mb downstream of the warming over Asia.

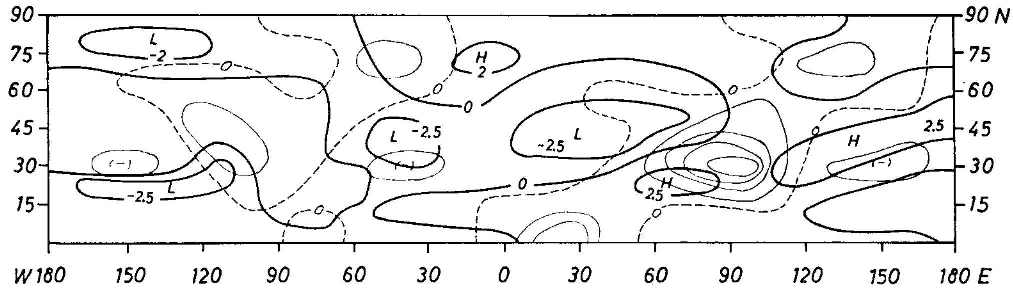

Fig. 6. Perturbation of the 400 mb height (dm) due to the longwave heating for January.

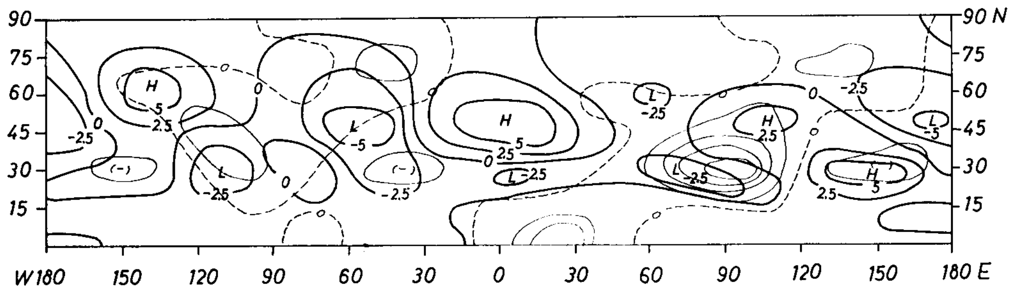

Fig. 7. Perturbation of the 400 mb height (dm) due to the combined sensible heat, latent heat and longwave radiation forcing for January.

The northward transport of westerly momentum at 400 mb shows a maximum of 4 ms^{-1} at 20° N but is weak elsewhere as are the other transports.

(d) Shortwave radiation

At present, no reliable charts of the mean absorption of shortwave radiation are available. In principle, we could have tried to compute the heating due to absorption of shortwave radiation from charts of the planetary albedo and from charts of the shortwave radiation received at the earth's surface. However, absorption in the stratosphere must be treated separately and it has been felt that such a preparation of a chart of the shortwave absorption in the atmosphere was beyond the scope of this study. Hence, shortwave radiation is neglected.

(e) Composite solution due to the forcing by all heat sources

The composite solution for all heat sources is the superposition of the perturbations caused by the flux of sensible heat, the release of latent heat and by longwave radiation. Fig. 7 shows the composite geopotential perturbation at 400

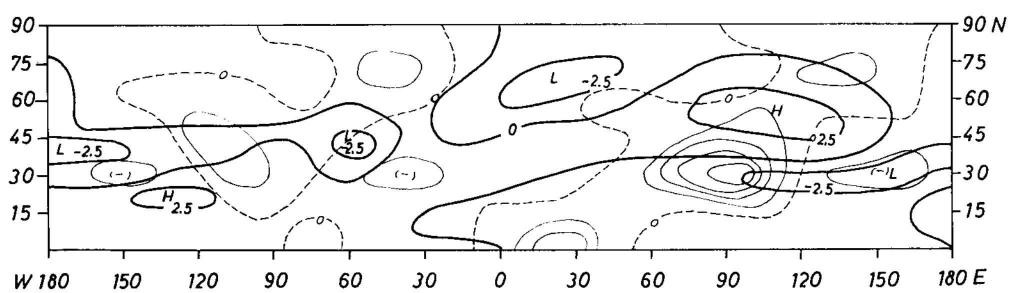

Fig. 8. Perturbation of the 800 mb height (dm) due to the combined sensible heat, latent heat and longwave radiation forcing for January.

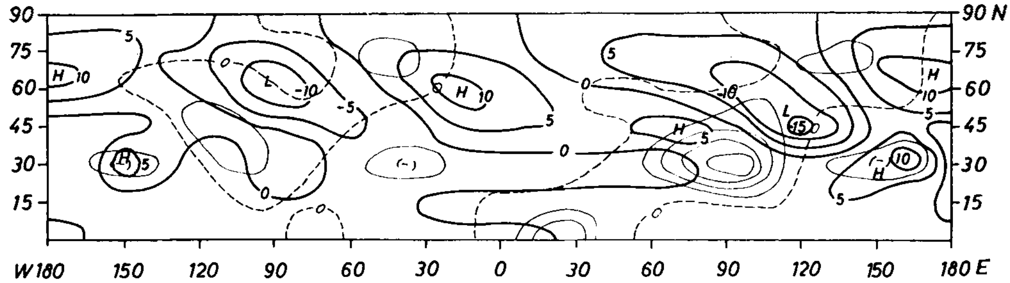

Fig. 9. Perturbation of the 400 mb height (dm) due to the combined forcing by the orography and all heat sources for January.

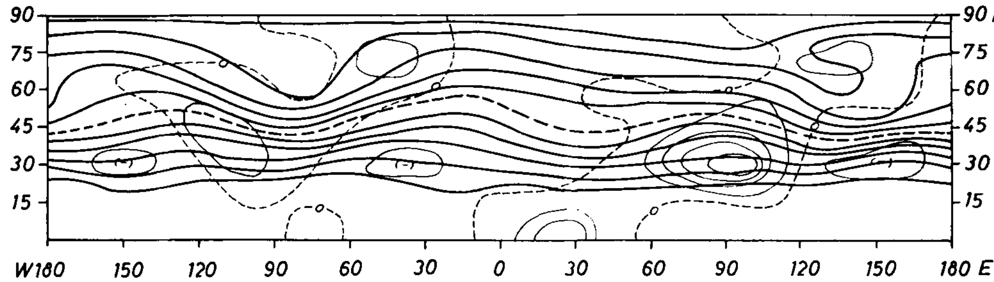

Fig. 10. The observed height of the 400 mb surface for January, with isolines every 100 m and the 700-m contour dashed. From Gates (1972).

mb. The pattern bears strong resemblance to the response to the release of latent heat. The longwave radiation reduces the amplitude of the composite response but the overall pattern is that due to the release of latent heat and the flux of sensible heat from the earth's surface.

Fig. 8 shows the composite perturbation geopotential at 800 mb. Both the low over the western Atlantic and the high north of the Himalayas are found at 800 mb as well as at 400 mb. On the other hand, the response at 800 mb over the eastern Atlantic, near 150° E, 30° N and near 110° W, 30° N is opposite to that at 400 mb.

The transports of momentum and sensible heat are strong and northward between 10° N and 35° N. North of 40° N, we observe a southward transport of westerly momentum ($\gtrsim -3$ ms^{-1}) at 400 mb. All other transports are rather weak.

(*f*) *Orographically forced response*

The response to the forcing by the orography has been discussed in I. At 400 mb, ridges are seen above the western part of the Himalayas, over the Atlantic (centre at 30° W, 50° N) and a fairly strong high extends from Asia to Alaska (center at 170° E, 65° N). Low pressure is

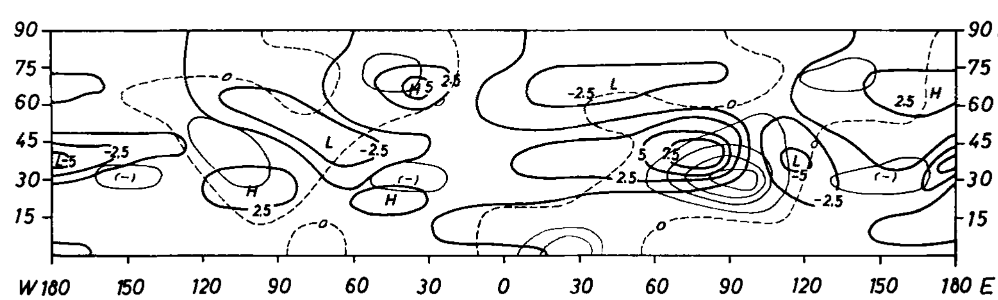

Fig. 11. Perturbation of the 800 mb height (dm) due to the combined forcing by orography and all heat sources for January.

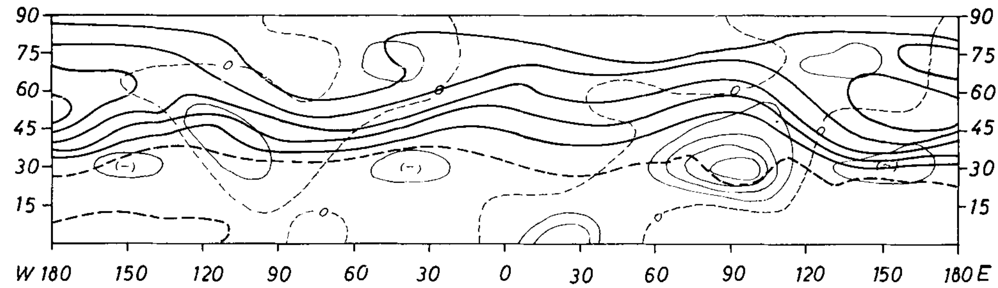

Fig. 12. The observed height of the 800 mb surface for January, with isolines every 50 m and the 2 000-m contour dashed. From Gates (1972).

found over Canada and to the northeast of the Himalayas. The response is almost the same at 800 mb, however with half the strength.

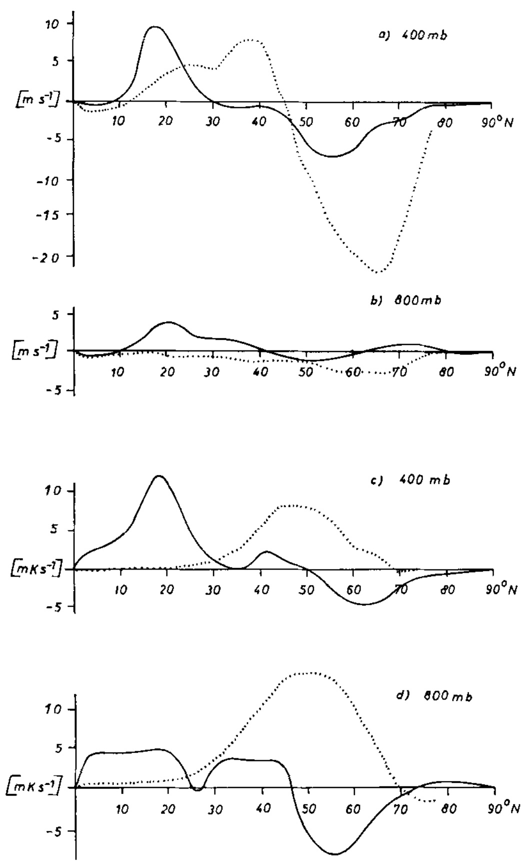

Fig. 13. The northward transport of westerly momentum (*a*, *b*) and of sensible heat (*c*, *d*) by the standing waves as given by the primitive equation model (solid) and as observed (dots) for January (Oort & Rasmusson, 1971).

(*g*) *Response to topographical and thermal forcing*

Fig. 9 shows the perturbation geopotential at 400 mb when orography and all available heat sources are included. The observed height of the 400 mb surface for January is shown in Fig. 10. The verification of Fig. 9 against Fig. 10 is good. All major observed ridges and troughs are also found in Fig. 9. In both figures, we have a ridge off the west coast of North America with a SE–NW tilt of the crest, a trough over the northeastern part of North America, a ridge over the eastern Atlantic, a weak ridge on the windward side of the Himalayas and a strong trough over Northeast Asia. Even the amplitudes of the standing waves compare favourably.

Discrepancies are seen near 30° E where the weak trough in Fig. 10 is badly represented in Fig. 9 and also near 180° E, 60° N where the American ridge is placed west of the observed position by the linear model.

Comparing Fig. 8 to Fig. 9 we may conclude that the ridge on the windward side of the Himalayas and the strong trough over eastern Asia are orographically induced. On the other hand, the response due to the heat sources plays an almost dominant role over North America and leads to a good verification of the ridge over the Atlantic. Also, the small cell of high pressure east of the Himalayas is due to the heat sources. The heat sources create an Aleutean low which is, however, overpowered by the orographically induced ridge in this area. Manabe & Terpstra (1975) have performed a set of numerical experiments by use of a general circulation model with and without mountains in order to identify the effects of mountains upon the general circulation in January. They found that the mountain model reproduced fairly realistically the troughs in the lee of the Rocky Mountains and of the Himalayas and created a reasonable ridge over the Atlantic whereas the model without mountains failed to show these features. Our results corroborate the findings of Manabe and Terpstra with respect to the effects of the Tibetan plateau but the ridge over the Atlantic is partly induced by the heat sources according to linear theory. Indeed, the Atlantic ridge is placed too far to the west in the mountain experiment of Manabe & Terpstra (Figs. 4.1*a–c* of their paper) just as predicted by the linear theory for orographically induced perturbations. Manabe and Terpstra point out that the maximum heating off the east coast of North America is much weaker in their experiments than in the charts of Budyko (1963). This shortcoming may be responsible for the absence of a ridge over the Atlantic in their experiment without mountains. At 800 mb (Fig. 11), the Aleutean high is too strong but the overall verification against Fig. 12 is satisfactory.

Fig. 13 shows the northward transport of heat and momentum by the standing waves as given by our model (solid) and as observed (dots). At 400 mb, the computed heat transport shows the main features of the observed transport, i.e. northward transport south of $\sim 40°$ N and southward transport north of 40° N. At 800 mb, the computed and the observed transport is extremely weak.

The momentum transport at 400 mb is simulated rather badly since the maximum of northward transport is placed considerably too far to the south as is the maximum of the southward transport. The simulation is better at 800 mb.

In all, we can state that the primitive equation model gives at least the basic features of the observed transports, i.e. northward transport in the southern part of the hemisphere and southward transports in the northern part. Furthermore, the order of magnitude of the computed transports is correct. General circulation models do hardly better (see Fig. 6.1 of Manabe & Terpstra, 1974).

Acknowledgement

The author is grateful to Prof. Raschke for comments on the radiational heating problem.

REFERENCES

Budyko, M. I. 1963. Atlas of the heat balance of the earth. Gidrometeorizdat, Moscow, 69 pp.

Egger, J. 1976. The linear response of a hemispheric two-level primitive equation model to forcing by topography. *Mon. Weath. Rev.*, 104, 351–364.

Gates, W. L. 1972. The January global climate simulated by the two-level Mintz–Arakawa model: a comparison with observation. RAND, Santa Monica, California, 107 pp.

Manabe, S. & Terpstra, T. B. 1974. The effects of mountains on the general circulation of the atmosphere as identified by numerical experiments. *J. Atmos. Sci. 31*, 3–42.

Möller, F. 1951. Vierteljahreskarten des Niederschlags für die ganze Erde. *Petermanns geographische Mitteilungen 95*, 1, 1–7.

Newell, R. E., Vincent, D. C., Dopplick, T. G., Ferruzza, D. & Kidson, J. W. 1969. The energy balance of the global atmosphere. The global circulation of the atmosphere. *Roy. Met. Soc. London 42*, 91.

Oort, A. H. & Rasmusson, E. M. 1971. Atmospheric circulation statistics. *NOAA Prof. Pap. 5*, NOAA, Rockville, Md.

Raschke, E., Von der Haar, T. H., Pasternak, M. & Bandeen, W. R. 1973. The radiation balance of the earth–atmosphere system from nimbus 3 radiation measurements. *NASA Technical Note D-7249*, Washington, D.C., pp. 73.

Saltzman, B. 1965. On the theory of winter-average perturbations in the troposphere and stratosphere. *Mon. Weath. Rev. 93*, 195–211.

К ТЕОРИИ СТАЦИОНАРНЫХ ВОЗМУЩЕНИЙ В ТРОПОСФЕРЕ

Изучается линейная стационарная реакция полусферной двухуровенной модели, основанной на примитивных уравнениях, на возбуждающее воздействие тепловых источников и топографии. Реалистичное возбуждение рассматривается для января, когда зональное изменение эффекта скрытой теплоты конденсации и обычного нагревания превалирует над радиационным нагреванием. Обсуждается реакция на каждый из этих источников и делается попытка понять вычисленные поля с помощью простой квазигеострофической теории. Совместное топографическое и термическое возбуждение вызывает неподвижные волны, которые хорошо согласуются с наблюдениями. На уровне 400 *мб* гребень на наветренной стороне Гималаев и ложбина над северо-восточной Азией, по-видимому, наводятся орографией, тогда как источники тепла играют почти доминирующую роль над Северной Америкой и определяют положение гребня над Атлантикой. На уровне 800 *мб* линейная модель не воспроизводит Алеутскую депрессию, однако, она является довольно удовлетворительной в других местах. Обсуждается перенос к северу тепла и количества движения неподвижными волнами.